Evaluation of Electromagnetic Interference from a Cellular Telephone with a Hearing Aid

K. Caputa, M. A. Stuchly, *Fellow, IEEE*, M. Skopec, H. I. Bassen, P. Ruggera, and M. Kanda

***Abstract*—In a collaborative effort, electromagnetic interference (EMI) is evaluated from a global system for mobile communication telephone with one model of a hearing aid used in the ear canal. Since the electromagnetic fields cannot be measured in the ear canal, a reliable method of their modeling with the finite-difference time-domain method is established. Very good agreement has been achieved between the measured and computed electric and magnetic fields in free space in very close proximity to the telephone. Subsequently, electric and magnetic fields in the ear canal are computed for two models of the ear, and three positions of the telephone. The computed fields are compared with the acoustic measurements for a small number of humans subjected to the EMI test.**

***Index Terms*—Cellular telephone, EMI, hearing aid.**

I. INTRODUCTION

CELLULAR telephones such as the global system for mobile communication (GSM) and personal communication services (PCSs) are well known to cause electromagnetic interference (EMI) with hearing aids. The main source of the EMI is the amplitude modulation in the acoustic range due to the time-division multiple access (TDMA) and to a lesser extent the code-division multiple access (CDMA). In the case of the TDMA, a frequency of 217 Hz and its harmonics are present in European systems, and 50 Hz and its harmonics in North American systems. For the CDMA transmitter, at full output power, there is no significant amplitude modulation, and at variable power rates the EMI spectrum resembles that of white noise [1]. The magnitude of the acoustic interference depends on several parameters of the telephone and aid [1]–[3]. For a given type of the telephone, the level of EMI induced sound pressure levels (SPLs) vary by more than 40 dB, depending on design of the hearing aid [1]. Similar levels of interference have been observed for hearing aids used in both microphone and telephone coil modes of operation. In the coil mode, the hearing aid responds only to magnetic fields produced by the telephone [1]. More often though, hearing aids are set to the microphone operation. Moreover, similar levels of interference in both modes of operation implicate either both electric and magnetic components of the telephone field or only the magnetic component. Thus, for a given hearing aid and telephone, the EMI depends on the fields in the location of the hearing aid.

Earlier numerical modeling has shown that the electromagnetic fields from a cellular telephone are very different in the ear canal compared to those in free space [4]. These early results refer to a generic telephone consisting of a monopole on a metallic box, and vertical placement of the handset next to the head. Both electric and magnetic fields vary much more rapidly with distance inside the ear canal than in free space. Different spatial components of the fields are produced in and around the ear from those around the telephone in free space.

As an extension of previous work, in this paper we report on a collaborative effort related to EMI with hearing aids. This paper is aimed at a comparison of the electromagnetic fields and levels of acoustic interference for a hearing aid placed in the ear. Laboratory measurements of the electric and magnetic fields were obtained from the laboratories of Motorola, Plantation, FL. Extensive numerical modeling of fields in free space and in the ear canal was performed at the University of Victoria, Victoria, BC, Canada. Acoustic measurements, also in free space and in the ear canal of a few volunteers, were obtained at the Food and Drug Administration, Rockville, MD. All investigations are for the same GSM telephone.

II. EXPERIMENTAL AND COMPUTATIONAL METHODS

A. Measurement of Fields Around a Telephone

Electric and magnetic fields have been measured using an automatic scanning system and miniature free-space E- and H-field probes. The probes consist of three small antennas and give a total magnitude of the field measured. External diameters are 6.9 and 5.9 mm for the electric- and magnetic-field probes, respectively. The scans are performed in four planes spaced 10–40 mm from the center of the telephone earphone. The frequency is 902.4 MHz (center of the transmit band) and the power output is set to the test mode. The manufacturer's specifications for the probes indicate $\pm 12\%$ measurement uncertainty. However, spurious reflections in the laboratory environment produced greater errors, estimated at 20%.

B. Modeling Method

Telephone shape and position with respect to the head are shown in Fig. 1. The schematic drawing [see Fig. 1(a)] shows the actual shape of the handset with its antenna, as well as the metallic parts that are included in the model. The handset placement simulates the most common-use position. The earphone

Manuscript received January 31, 2000; revised February 20, 2000. This work was supported in part by Bell Wireless Alliance and Telus under a contract. The work of K. Caputa and M. A. Stuchly was supported in part by the NSERC Industrial Research Chair Program.

K. Caputa and M. A. Stuchly are with the Department of Electrical and Computer Engineering, University of Victoria, Victoria, BC, Canada V8W 3P6.

M. Skopec was with the Food and Drug Administration, Rockville, MD 20852 USA. She is now with the National Institutes of Health, Bethesda, MD 20892 USA.

H. I. Bassen and P. Ruggera is with the Food and Drug Administration, Rockville, MD 20852 USA.

M. Kanda is with Motorola, Plantation, FL 33322-9947 USA.

Publisher Item Identifier S 0018-9480(00)09709-X.

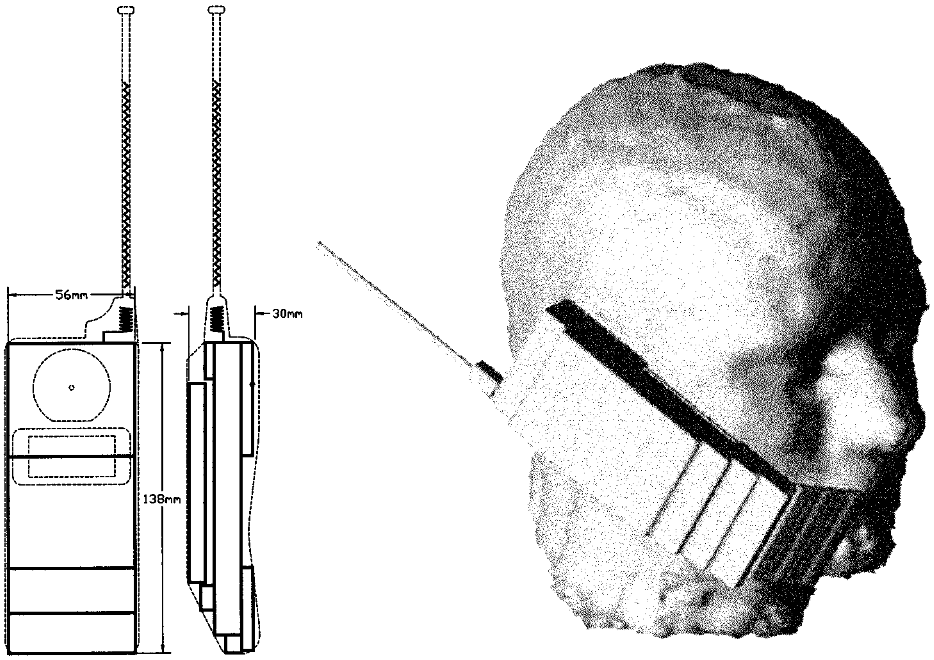

(a) (b)

Fig. 1. (a) Engineering drawing of the telephone (dashed and solid lines) and its model (solid line). (b) External view of the head of the telephone model in a common-use position.

faces the auditory canal, the microphone is placed close to the mouth, and the handset body is in contact with the cheek.

An anatomically correct magnetic resonance imaging (MRI)-derived model of the human head is used with over 30 tissues identified. The model resolution is 1.1 mm $\times$ 1.1 mm in horizontal directions and 1.4 mm in the vertical direction down to the upper jaw and lower resolution (3.6 mm) below. Special care has been devoted to preserve the outer and inner ear anatomy. Two models of the outer ear (pinna) are available. One model with the ear compressed represents the ear shape with a telephone tightly pressed to the ear. In the other model, the ear retains its nonconstricted shape, as obtained from accurate segmentation of MRI images. As described earlier, a computer-based tool is used to locate test points for recording computed electromagnetic fields in the ear canal [4]. The recorded fields may not necessarily be exactly in the center of the canal, as they are computed in the center of the grid. These fields are recorded as a function of distance from the entrance of the ear canal and along a curved path of the canal.

Computations are performed using the finite-difference time-domain (FDTD) method [5]. Two different FDTD codes are used, our own code and an *LC* code provided by the SGI, Mountview, CA.[1] The reason for two codes is to ensure reliable modeling of the helical antenna and computational efficiency. Our own code has graded meshes, thus facilitating reduction of computer resources for larger problems that include the human head. Additionally, this code allows us to properly maintain allocation of tissue electrical properties in a rotated head model. The helix is modeled as consisting of interconnected straight wire sections and loops similarly as elsewhere [6]. The antenna is modeled on a handset, whose dimensions of metallic parts are accurate. The handset box is covered with a dielectric material. Several test trials that have been performed indicate that such features such as curvature of plastic parts and small detail of the telephone do not change the electromagnetic fields by more than 1%. Thus, the telephone model consists of metal parts, shown in Fig. 1(a), covered with 1-mm dielectric of $\varepsilon_r' = 2.1$. A perfectly conducting layer (PML) [7] terminates the computational space. An excellent agreement has been obtained for the antenna on the handset resonant frequency and impedance by both codes with two methods of antenna excitation.

[1]K. Thomas, *LC User's Guide, Version 2.7,* Feb. 1999. [Online]. Available: http://www.lc.cray.com

The total output power from the antenna is computed from the radiated power for free space and as a sum of the total radiated and total absorbed power in the tissue for the telephone next to the head [8]. The grid resolution varies from 1–4 mm. Graded meshes are used with a fine grid to model the antenna and its vicinity and the ear region. A coarser resolution is used further away from the area of interest. A time-shifted Gaussian pulse excites the antenna. Virtually the same results have been obtained with two types of excitation. They are a 50-Ω coaxial line and an air gap with a 50-Ω source.

In the FDTD modeling, the handset is aligned with the coordinate system. Appropriate measures are taken to maintain the head anatomy after the rotation. The handset placement closely simulates that used in the acoustic measurements. Due to differences in ear shapes and telephone placement, several modifications of the placement are investigated. Also, as mentioned earlier, two pinna shapes are considered. The hearing aid itself is not included in the modeling. This is justified by the fact that exposure fields are normally defined without a device in place.

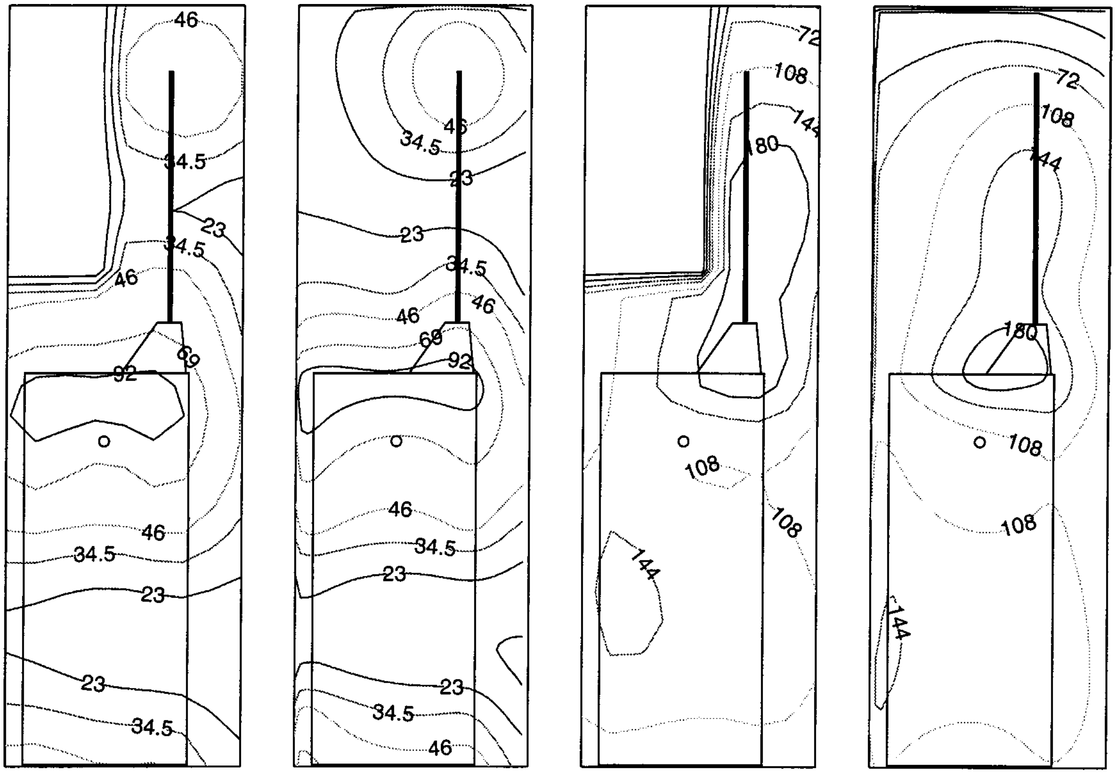

(a) (b) (c) (d)

Fig. 2. Electric fields in volts per meter. (a) Measured, (b) computed, and magnetic fields in milliampere per meter. (c) Measured. (d) Computed. All values are in free space, 1 cm from the earphone. Antenna extended.

C. Acoustic Measurements

The hearing-aid EMI is evaluated by measurements of RF-induced SPL. Tygon tubing connects the hearing aid via an acoustic coupler to the SPL meter, as described in [1]. Measurements are performed for the hearing aid in free space and the ear canal. In both cases, the hearing aid is aligned with the center of the telephone earphone. The distance between the hearing aid and phone is 10 mm for both test positions (free space and telephone placed against the ear). Data has been obtained for three persons. Two separate measurement sets of ten samples are taken for each person.

When exposed to pulse-modulated fields from the GSM phone, an audio tone is induced in the hearing-aid acoustic output with a fundamental frequency of 217 Hz. The single frequency of 217 Hz in the SPL signal has been measured with a Bruel and Kjaer Type 2144 Frequency Analyzer to determine the SPL in dBA emitted by the hearing aid. The case of free-space exposure of the hearing aid is used as a reference level.

To obtain insight into the relationship between the RF magnetic-field strengths exposures from a cellular phone and the resulting acoustic SPL produced by the hearing aid, an additional experiment has been performed. An RF signal generator with GSM modulation imposed on its signal has been used to deliver a simulated GSM phone signal of a few milliwatts to an RF amplifier. The amplifier delivers higher power GSM-modulated RF signals to a half-wave dipole antenna through a coaxial cable. The hearing aid under test is placed at the center of the dipole (the region where the maximum magnetic field exists). RF power into the dipole has been adjusted to produce SPL levels that exist over the entire range of experimental values obtained with the GSM test telephone. These values included those of the hearing aid in the ear of three test subjects.

III. Comparison of Measured and Computed Fields

Electromagnetic fields are extremely difficult, if not impossible, to measure accurately in the ear canal using presently available field probes. Only computed fields can be used for comparison of their strength with levels of measured acoustic interference for hearing aids placed in the ear canal. An agreement between the computed and measured magnitudes of the electric field inside models of head has previously been reported (e.g., [9]). However, it is recognized that correct modeling of the antenna and handset are critical to achieve good agreement. That is why we used two FDTD codes to verify the antenna modeling and test if detailed representation is needed. We compare magnitudes of both fields (magnetic in addition to electric) in free space near to the antenna, where the fields are spatially very nonuniform. With the measurements and computations performed in different laboratories, we thus presume that the computed fields in the ear are accurate within the limits of uncertainties associated with the methods used. Figs. 2 and 3 present detailed maps of the measured and computed fields in a plane parallel to the handset, 1 cm away for the retracted and extended antenna. It should be noted that the measured fields have not been scanned in the areas on the upper left-hand side corner of the planes. The same output power of the telephone (test mode) is used in all measurements and computations. Good agreements are apparent for both the electric and

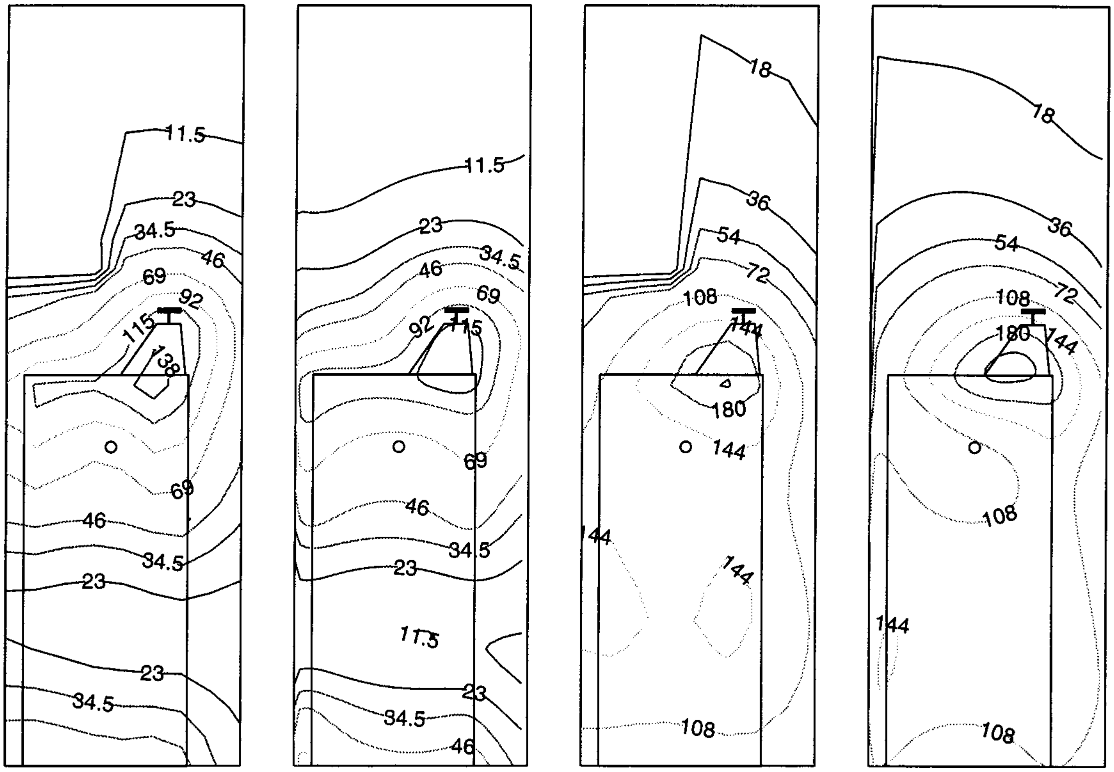

(a) (b) (c) (d)

Fig. 3. Electric fields in volts per meter. (a) Measured, (b) computed, and magnetic fields in milliampere per meter. (c) Measured. (d) Computed. All values are in free space, 1 cm from the earphone. Antenna retracted.

TABLE I
COMPARISON OF THE FIELDS MEASURED AND COMPUTED IN FREE SPACE CLOSE TO THE TELEPHONE (ALL DIFFERENCES ARE IN PERCENTAGES)

Antenna	Extended						Retracted					
Component	E-field			H-field			E-field			H-field		
Separation	Δ_R	Δ_M	Δ_{STD}	Δ_R	Δ_M	Δ_{STD}	Δ_R	Δ_M	Δ_{STD}	Δ_R	Δ_M	Δ_{STD}
1 cm	5.3	13.5	28	0.1	11.4	7.2	0.7	16	21	2.8	12	6.5
2 cm	1.7	8.6	15	0.3	9.2	23	1.9	11	24	0.8	9.7	21
3 cm	2.5	6.4	11	0.4	7.6	27	3.2	9.1	28	2.0	7.8	25
4 cm	2.1	6.8	13	0.3	6.9	27	3.7	10	33	2.5	7.8	26

magnetic fields. Table I gives more quantitative global comparisons for four planes where measured data are available. These data refer to a test area of 9 cm $\times$ 16 cm, sampled in a grid of 10-mm (total of 170 points). The test area is rectangular and extends up to the region where the measurements are not taken (Figs. 2 and 3). Three measures of error are used. One of the measures is a relative difference (Δ_R) between mean measured and computed fields within the test area. The second measure is the mean value of absolute error (Δ_M) defined as

$$\Delta_M = \text{mean}\left[\frac{2|F_{mi} - F_{ci}|}{F_{mi} + F_{ci}}\right] \tag{1}$$

where F_{mi} and F_{ci} are measured and computed fields, respectively, in each point within the test area. The final measure is the standard deviation

$$\Delta_{\text{STD}} = \left[\text{mean}\,\frac{2|F_{mi}^2 - F_{ci}^2|}{|F_{mi}^2 + F_{ci}^2|}\right]^{1/2}. \tag{2}$$

Examination of data in Table I indicates a reasonably close agreement between the computed and measured electric and magnetic fields. This agreement for 1-cm plane separation is within the surface area where the hearing aid is placed in the acoustic measurements. All the mean fields (Δ_R) are remarkably close to each other. Larger differences up to 16% are in mean values of relative absolute differences (Δ_M) in each point. Even larger Δ_{STD} can be noted, as this measure emphasizes differences in single points. The differences of the magnitude observed are entirely expected in view of the errors associated with measurements alone. Uncertainties associated with computations are more difficult to estimate. With the size of the grid used and closeness of results obtained with two FDTD codes, the method is accurate at least within 2% (or better). However, there are errors associated with modeling details of the antenna and handset. These errors are quite difficult to assess quantitatively. However, the good agreement between the measurements attests to reasonable modeling of the device. Our tests of telephone representation have indicated a lack of sensitivity to small details of the dielectric parts of the handset. A relative insensitivity to modeling of fine details of the handset has been also reported in [10] for power deposition

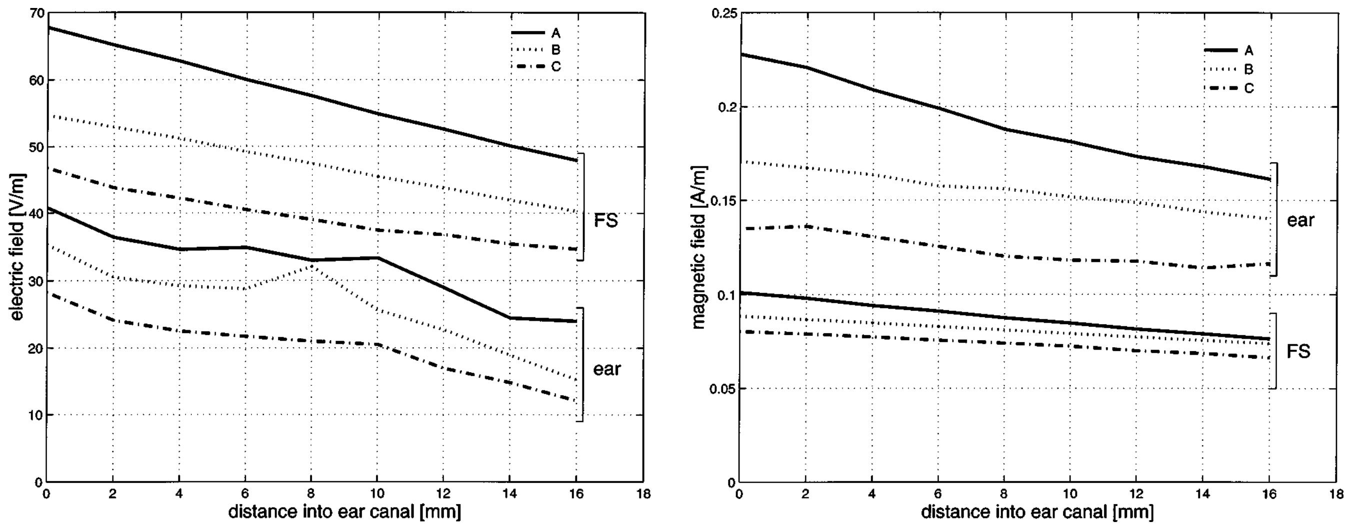

(a) (b)

Fig. 4. (a) Electric- and (b) magnetic-field magnitude in free space (FS) and the ear canal (E) for the compressed ear-model and various positions of the telephone. Antenna extended. A: the center of earphone in the reference point [see Fig. 1(b)]. B: the earphone 4 mm away from the ear canal, and aligned with the reference point. C: the earphone 12 mm away from the ear canal, and aligned with the reference point.

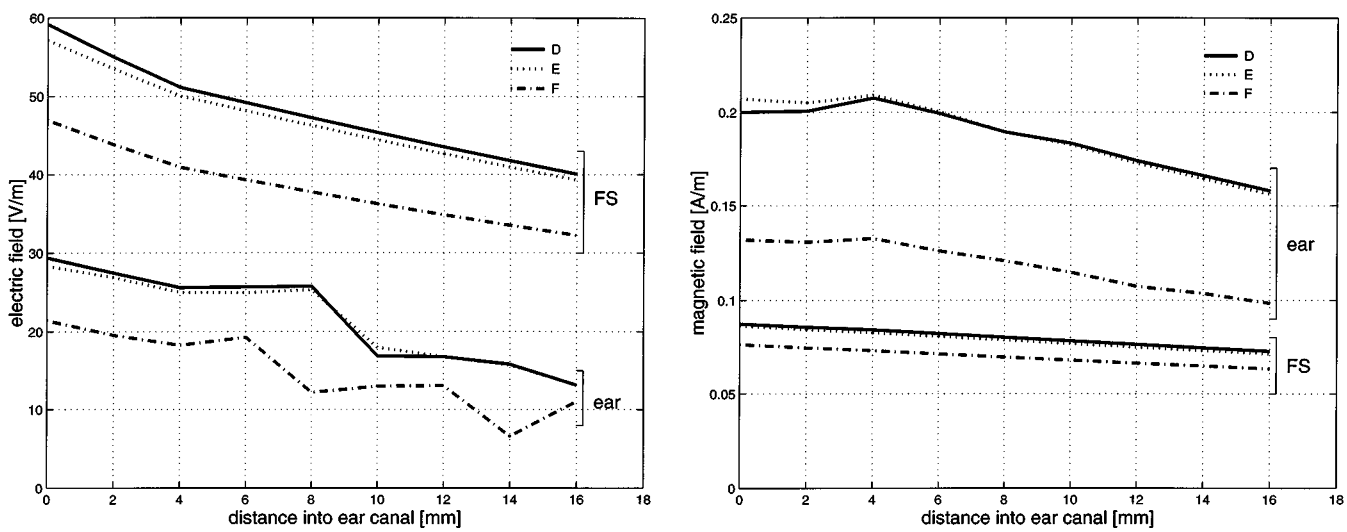

(a) (b)

Fig. 5. (a) Electric- and (b) magnetic-field magnitude in free space (FS) and the ear canal (E) for the normal-shape ear model and various positions of the telephone. Antenna extended. D: telephone shifted 8 mm toward the mouth. E: the center of earphone in the reference point [see Fig. 1(b)]. F: the earphone 8 mm away from the ear canal, and aligned with the reference point.

in the head. On the other hand, it needs to be stressed that correct representation of the antenna is essential. Data in Table I also indicates that values of Δ_M are generally smaller in planes further removed from the telephone. With the dimensions of the measurement probes, particularly for the electric field, there is a possibility of coupling of the sensor antenna with the handset.

IV. Fields in the Ear Canal

Figs. 4 and 5 show the magnitude of the electric and magnetic fields for two models of the ear (pinna). These magnitudes are shown close to the center of the ear canal. It needs to be noted that the ear canal is not aligned with any axis of the coordinate system, and does not proceed along a straight line. The distance shown on the abscissa is measured from an entrance into the auditory canal. The center of the entrance in the auditory canal is at the reference point. The free-space curves correspond to the magnitude of the fields without the head, but with the cellular telephone in the same position. For each ear model, in addition to the standard placement of the telephone, as in Fig. 1(b) (and acoustic tests), results for two other placements are illustrated.

One general observation is that the magnitudes of the electric fields are attenuated in the ear canal, while the magnitudes of the magnetic fields are enhanced. The result for the magnetic field may be surprising; however, it is in agreement with the previously reported results for a monopole antenna on a handset [4]. The head in the near field of the handset antenna changes the input impedance and performance of the antenna. Furthermore, the fields are scattered within the heterogeneous model of the head. As a result, components of the field appear that are not present in free space. Overall, each field component may vary quite rapidly inside the ear canal, as observed in [4], as well as in

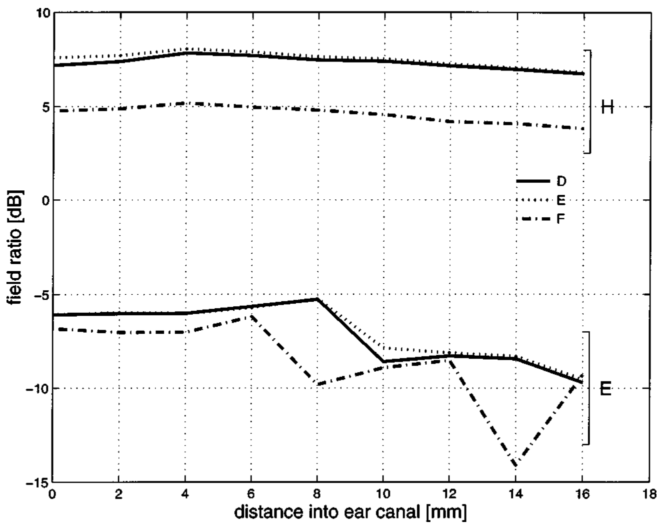

Fig. 6. Ratio of the electric (E) fields and magnetic (H) field in the ear canal to those in free space for the flattened ear model and various positions of the telephone. Antenna extended. A: the center of earphone in the reference point [see Fig. 1(b)]. B: the earphone 4 mm away from the ear canal, and aligned with the reference point. C: the earphone 12 mm away from the ear canal, and aligned with the reference point.

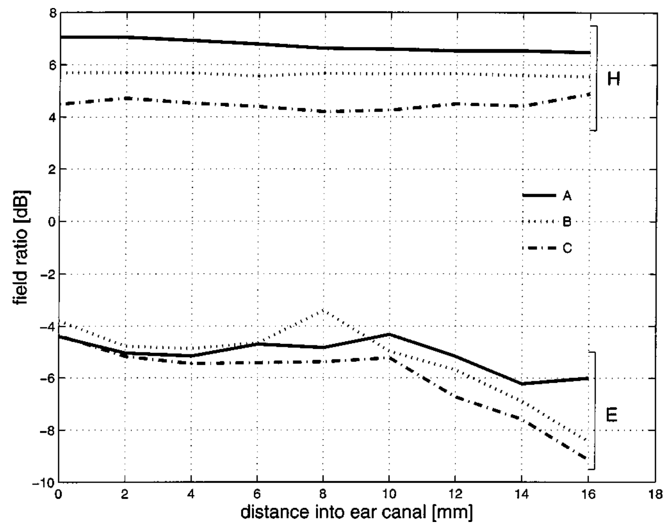

Fig. 7. Ratio of the electric (E) fields and magnetic (H) field in the ear canal to those in free space for the normal-shape ear model and various positions of the telephone. Antenna extended. D: telephone shifted 8 mm toward the mouth. E: the center of earphone in the reference point [see Fig. 1(b)]. F: the earphone 8 mm away from the ear canal, and aligned with the reference point.

this paper. The magnitude of the total field usually changes more smoothly. A few rapid changes of the electric field in Figs. 4 and 6 are most likely due either to the test point being close to the canal wall or a rapid change in magnitude of one field component.

Certain self-consistent features of the field behavior in the ear canal can be observed. One of them is that, for the electric fields, the order of the curves for the field magnitude in the ear canal, in general, corresponds to that of the field magnitude in free space. The relationship is not evident to the same extent for the magnetic fields, but generally reasonable. The behavior of the magnetic fields is reasonable in view of the free-space field distribution and previous report results [4].

The ratios of the electromagnetic fields in the ear canal and free space are given in Figs. 6 and 7 for the two models of the ear. For both ear models, the magnetic-field ratios change little with distance into the ear. The variations are greater for the electric-field ratios, which is consistent with data shown in Figs. 4(a) and 5(a). On the other hand, the electric field close to 10–12 mm into the ear (where the hearing aid is located) varies little. For the placements of the handset, as in Fig. 1(b), the magnetic-field ratios are 6.7 and 7.5 dB for the two ear models.

V. EMI EVALUATION

The acoustic measurements indicated that, when the hearing aid was placed in the ear of three subjects, the average SPL increased by 7.4 dBA, with a standard deviation of 0.77 dBA compared to the reference case. The fact that the SPL increases, relative to free-space exposure, when the hearing aid is placed in the ear of a person, is consistent with an increased magnetic-field strength. The relationship between the output of the hearing aid, i.e., 217-Hz acoustic SPL and the RF power delivered to the dipole, is shown in Fig. 8. As can be seen, the relationship for this hearing aid, as the RF power increased, was nonlinear. As RF power was increased in 3-dB increments, the hearing-aid

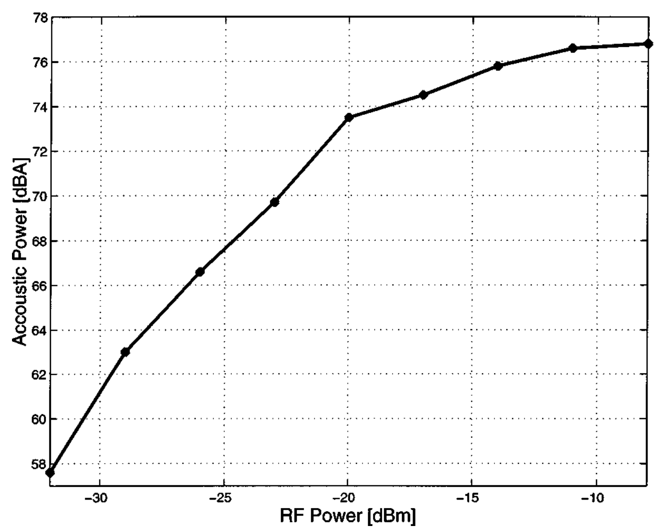

Fig. 8. Acoustic power at 217 Hz as a function of the RF power, data used to normalize the hearing aid SPL measurements. $S1$, $S2$, and $S3$ refer to the test subject number.

output SPL increased, but at higher RF levels the hearing-aid SPL appeared to saturate, and the increases in output SPL were lower for each subsequent 3-dB increase in RF power. The absolute SPL was measured for levels corresponding to the values occurring when the phone was place 10 mm away from the three human subjects ($S1, S2, S3$). In order to minimize feedback, the hearing-aid gain was adjusted for each subject. This accounted for the different ranges of SPL levels that were recorded for each of the subjects.

VI. CONCLUSIONS

A comprehensive evaluation of EMI has been performed for one telephone and one hearing aid used in the ear. The evaluation has consisted of electromagnetic measurements and computations and acoustic measurements. The ratios of the electromagnetic fields in the ear canal and free space are compared to the ratios of the measured interference levels (SPLs at 217 Hz) with the hearing aid in the ear of test subjects and free space. Since the electromagnetic field in the ear canal cannot be measured, reliability of their numerical modeling with the FDTD method has been established by comparing the measured and computed fields in the close proximity of the telephone. The telephone modeled has a complex helical antenna, whose proper modeling is critical.

For the telephone and hearing aid investigated, the quantitative results of the acoustic tests correlate well with the ratio of the magnitudes of the magnetic fields in the auditory canal and free space. Our data does not unequivocally indicate that the electric field does not play any role in the EMI observed. However, the acoustic levels are higher for the hearing aid in the ear than in free space. The magnitudes of the increase in SPL correlates reasonably well with larger magnetic fields. There is a direct avenue for coupling of magnetic fields as the hearing-aid microphone contains a coil. On the other hand, a visual examination of the hearing aid investigated has also revealed other wires, some of them forming loops.

There is variability in both acoustic and electromagnetic data. The ratios of the magnitude of electromagnetic fields in the ear and free space vary quite a lot depending on the ear shape and placement of the handset. Directional field components vary even more. The ratios of the magnetic fields for the two ear shapes for telephone and hearing-aid locations corresponding to those of the acoustic test are about 7 dB. This compares well with an average normalized SPL of 7.4 dB. Our data point out that it may be possible to predict hearing-aid SPL based on magnetic-field strength. However, other factors must be considered before any general conclusions can be drawn. These include the gain setting of the hearing aid, the absolute SPL produced by the hearing aid, and the absolute RF power level at a location of the hearing aid.

Acknowledgment

The authors thank Dr. W. Ansbacher, British Columbia Cancer Agency, Victoria, BC, Canada, for accurate imaging of the handheld telephone, which allowed us to model properly its internal structure and antenna in our FDTD simulations.

References

[1] M. Skopec, "Hearing aid electromagnetic interference from digital wireless telephones," *IEEE Trans. Rehab. Eng.*, vol. 6, pp. 235–239, Feb. 1998.

[2] F. K. Kuk and K. H. Nielsen, "Factors affecting interference from digital cellular telephones," *Hearing J.*, vol. 50, pp. 32–34, 1997.

[3] T. A. Victorian, "An update on digital cellular telephone interference and hearing aid compatibility," *Hearing J.*, vol. 41, pp. 53–60, 1998.

[4] M. Okoniewski and M. A. Stuchly, "Modeling of interaction of electromagnetic fields from a cellular telephone with hearing aids," *IEEE Trans. Microwave Theory Tech.*, vol. 46, pp. 1686–1693, Nov. 1998.

[5] A. Taflove, *Computational Electrodynamics: The Finite-Difference Time-Domain Method*. Norwood, MA: Artech House, 1995.

[6] J. S. Colbourn and Y. Rahmat-Samii, "Human proximity effects on circular polarized handset antennas in personal satellite communications," *IEEE Trans. Antennas Propagat.*, vol. 46, pp. 813–820, June 1998.

[7] J.-P. Berenger, "Perfectly matched layer for the FDTD solution of wave-structure interaction problems," *IEEE Trans. Antennas Propagat.*, vol. 44, pp. 110–117, Jan. 1996.

[8] M. Okoniewski and M. A. Stuchly, "A study of the handset antenna and human body interaction," *IEEE Trans. Microwave Theory Tech.*, vol. 44, pp. 1855–1864, Oct. 1996.

[9] Q. Yu, O. P. Gandhi, M. Aronsson, and D. Wu, "An automated SAR measurement system for compliance testing of personal wireless devices," *IEEE Trans. Electromagn. Compat.*, vol. 41, pp. 234–245, Aug. 1999.

[10] A. D. Tinniswood, C. M. Furse, and O. P. Gandhi, "Computations of SAR distributions for two anatomically based models of the human head using CAD files of commercial telephones and the parallelized FDTD code," *IEEE Trans. Antennas Propagat.*, vol. 46, pp. 829–833, June 1998.

K. Caputa, photograph and biography not available at time of publication.

M. A. Stuchly (S'71–SM'76–F'91), photograph and biography not available at time of publication.

M. Skopec, photograph and biography not available at time of publication.

H. I. Bassen, photograph and biography not available at time of publication.

P. Ruggera, photograph and biography not available at time of publication.

M. Kanda, photograph and biography not available at time of publication.